Electroless Synthesis of Cellulose-Metal Aerogel Composites

M. Schestakow,[1,a)] F. Muench,[2,a)] C. Reimuth,[2] L. Ratke,[1] and W. Ensinger[2]

[1]*Deutsches Zentrum für Luft- und Raumfahrt e.V., Institute of Materials Research, Linder Höhe, 51147, Köln, Germany*

[2]*Department of Materials and Geoscience, Technische Universität Darmstadt, Alarich-Weiss-Str. 2, 64287, Darmstadt, Germany*

An environmentally benign electroless plating procedure enables a dense coating of silver nanoparticles onto complex cellulose aerogel structures. In the course of the nanoparticle deposition, the morphological characteristics of the aerogel are preserved, such as the continuous self-supporting network structure. While achieving a high metal loading, the large specific surface area as well as the low density is retained in the cellulose-metal aerogel composite. Due to the interesting features of cellulose aerogel substrates (e.g. the accessibility of its open-porous network) and electroless plating (e.g. the possibility to control the density, size and composition of the deposited metal nanoparticles), the outlined synthetic scheme provides a facile and flexible route towards advanced materials in heterogeneous catalysis, plasmonics and sensing.

Porous noble metal nanostructures represent a remarkable material class composed of foams, sponges, aerogels, or nanotube assemblies.[1-5] Micro- and mesoporous metals produce highly active materials by means of their interfacial effects, and for the presence of macropores that provide efficient pathways for mass transport.[4] Metal aerogels or aerogel supported metal particle assemblies that combine an exceptionally high surface area with multiple pore sizes with a monolithic, self-supporting structure, have attracted special interest.[1,3,6-8] Due to the wide functionality range and high degree of efficiency that can be realized with nano-structured metals, this material class can meet emerging needs in energy storage,[9] catalysis,[10,11] sensor technology,[12,13] plasmonics[14] or drug delivery.[4,15] For instance, Ag nanoparticle (NP) deposits on polysaccharidic matrices address medical applications such as filtration, separation, drug delivery or plasmonics.[7,15-18] Typical synthetic strategies include the attachment of metal NPs to various template or substrate materials, sometimes followed by the template removal.[9,18-21] The results are highly active materials, but the procedures are often limited with regard to NP loading or production volume leading to reduced performance or lack of scalability.

[a)] Authors to whom correspondence should be addressed. Electronic mail: maria.schestakow@dlr.de, muench@ca.tu-darmstadt.de.

Functional aerogel metals can be prepared by a direct sol-gel approach[1] or by adding metal salts to the precursor solution.[7] Supported nano-metal architectures are mostly realized by reduction of adsorbed metal ions[17] or such methods as atomic layer deposition,[19,20] but none of these mention electroless plaiting (EP) of aerogels. EP is an easily scalable wet-chemical process that does not require complex instrumentation and can specifically be designed to meet green chemistry requirements.[22] Due to its conformal seed-based deposition mechanism, it is well suited for the homogeneous metallization of substrates enclosing complex pore networks.[2] By adjusting the deposition time, the amount of plated metal can be controlled. The method allows the deposition of numerous metals resulting in a variety of functionalities.[2,13,20-23] In contrast to conventional methods like in situ reduction or atomic layer deposition[17,19] EP is capable of creating dense NP coatings and thus enables considerably higher metal loading which is essential for electrical conductivity by percolation of conducting paths as well as for highly active catalysts and sensors.[2,11,13,24,25] Aerogels remarkably combine a high specific surface area, with high porosity and accessibility of the entire pore system in a monolithic solid and therefore, qualify for outstanding substrate materials. They are reported to effect responses in sensing, energy storage, and energy conversion orders of magnitude faster than other porous solids.[1] Porous noble metals architectures show outstanding performance in sensing applications.[12,19,26] Also, energy-related applications are conceivable.[9] To meet sustainability requirements without sacrificing performance, the use of biopolymers is promising. Cellulose is often favored for its abundancy and renewability as well as biocompatibility and flexibility in functionalization.[27] Cellulose nanocrystals or fibers efficiently support Pd or Ag NPs to serve as catalysts in e.g. reduction of 4-nitrophenol or electrooxidation of methanol.[11,17,18] Cellulose aerogels (CA) with such characteristics as the nano-felt-like structure, adjustable in density, porosity and mechanical properties can be prepared from easily recyclable aqueous salt hydrate melts.[27-31] In this task CA substrates have two main obstacles, namely (i) fracturing of the monolith in contact with typical, aqueous plating solutions due to strong capillary forces and (ii) sluggish diffusion of the reactive bath components to the inner areas. In overcoming these difficulties we were able to apply an EP procedure to CA substrate materials. Abrupt surface tension changes between different processing steps (seeding, washing, plating) was avoided by solely working with a solvent mixture and thus avoiding fracturing. The CA, prepared as described in,[29,30] was first soaked with pure ethanol, which was continuously replaced with water until a 1:2 ratio (ethanol:water) was reached. Intimate contact of the inner CA surface with the reagents was ensured by using a setup similar to column chromatography, in which the substrate monolith is flushed with the reaction solutions. The environmentally friendly nature of CAs is complemented by the EP reaction, which is performed at room temperature and uses unproblematic solvents, minimal amounts of inorganic tin salts, and non-toxic tartrate for Ag reduction.

First, the self-supported biopolymeric backbone is seeded with Ag NPs by the reaction of superficially bound Sn(II) ions with Ag(I) according to: Sn(II) + 2 Ag(I) → Sn(IV) + 2 Ag↓. The CA disks were flushed with a sensitization solution consisting of slightest $SnCl_2$ amounts and trifluoroacetic acid, which results in Sn(II) adsorption. After thorough washing, the gel was flushed with an activation solution ($AgNO_3$ and NH_3). This reaction is indicated by a change in color (white → brown). After a washing step, Ag deposition is performed by flushing the monolith with the plating solution which consists of a metal source ($AgNO_3$), a ligand (ethylenediamine), trifluoroacetic acid for pH adjustment and a reducing agent (potassium sodium tartrate). During this time, the gel turns darker, indicating the growth of the NPs and an increase of the Ag loading.

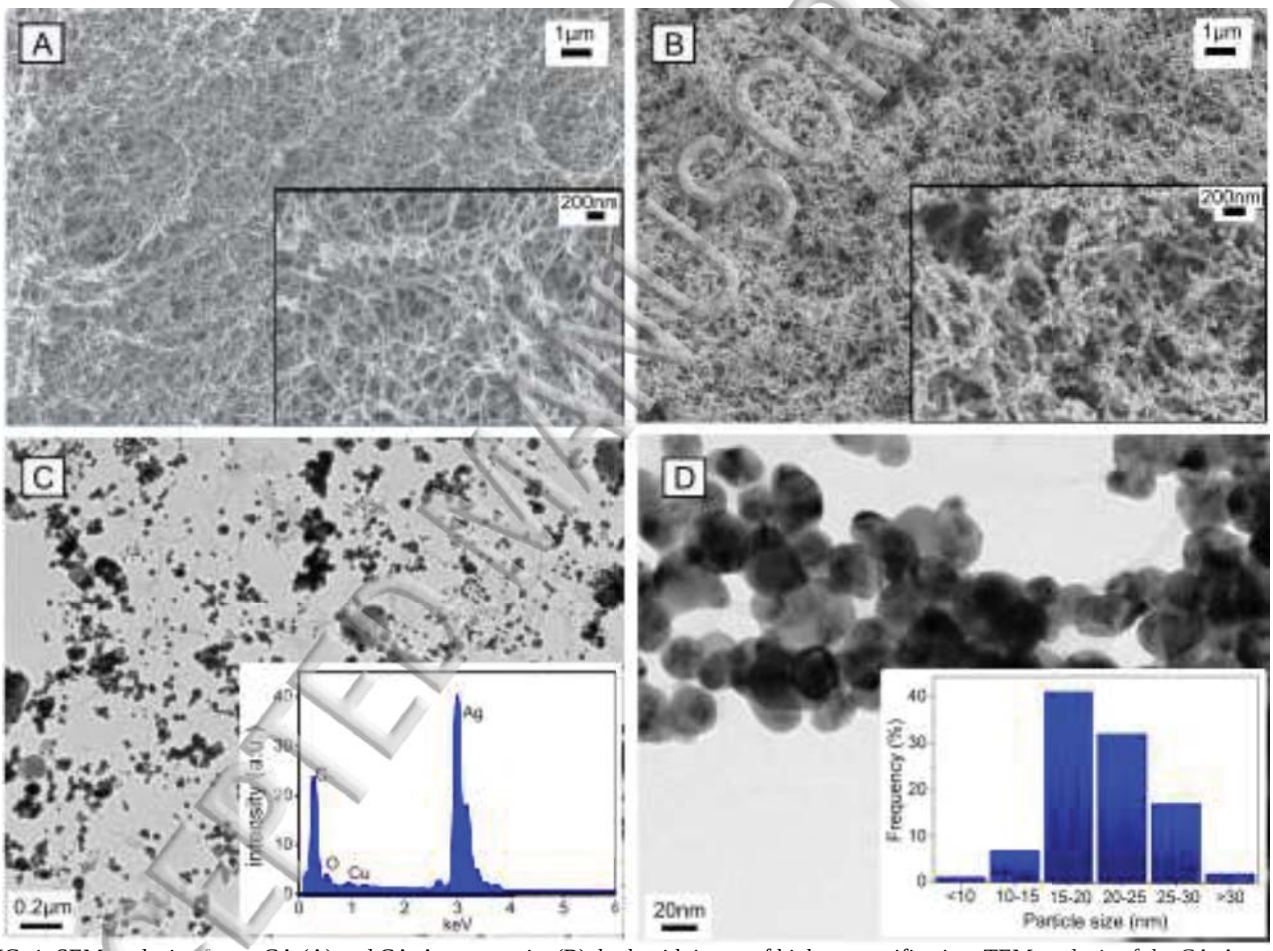

FIG. 1. SEM analysis of pure CA (A) and CA-Ag composite (B), both with insets of higher magnification. TEM analysis of the CA-Ag composite in different magnification (C, D). The insets show the EDX analysis (C; the Cu signal stems from the TEM grid) and the particle size distribution (D, n=200).

After EP, the gel was washed with ethanol subjected to supercritical drying (110 bar, 50°C for 24 h). The dry CA with 3 wt. % cellulose is white in color and deforms readily under compression, while the CA Ag-composite is less pliable and of black color.

Taking advantage of the regular cylindrical shape of the aerogel monoliths, the densities are gravimetrically determined to be 57 kg m^{-3} for the CA and 93 kg m^{-3} for the CA-Ag composite. Furthermore, the porosity of 97 % for CA is slightly reduced by Ag NP loading to yield 86 % in the composite. Both, the change in color and the increasing density indicate Ag NP deposition onto the aerogel. SEM analysis reveals the CA to consist of a 3D network of aperiodically distributed cellulose nano-fibrils (Fig. 1A). After EP, the structure remains fibrillar (Fig. 1B), whereas the pore size slightly decreases with Ag NP loading. The CA-Ag composite, confirmed by EDX analysis, inset Fig. 1C, appears highly homogeneous in Ag NPs size and distribution. However, from TEM image Fig. 1C the Ag NPs appear to be loosely mounted onto the fibrils, which may derive from sample preparation performed by grinding in liquid nitrogen. The most frequently occurring particle size is the range of 15-25 nm making 73 % in total (inset Fig. 1D) and thus, implying uniform growth times and conditions for the Ag NPs. Every fibril is covered with Ag NPs, indicating a very reliable and dense metal nucleation. We attribute this behavior to the polar surface chemistry of the cellulose. The ubiquitous presence of hydroxy groups provides a high density of bonding sites for the metal ions involved in the sensitization and activation steps, which in turn leads to an efficient template seeding.

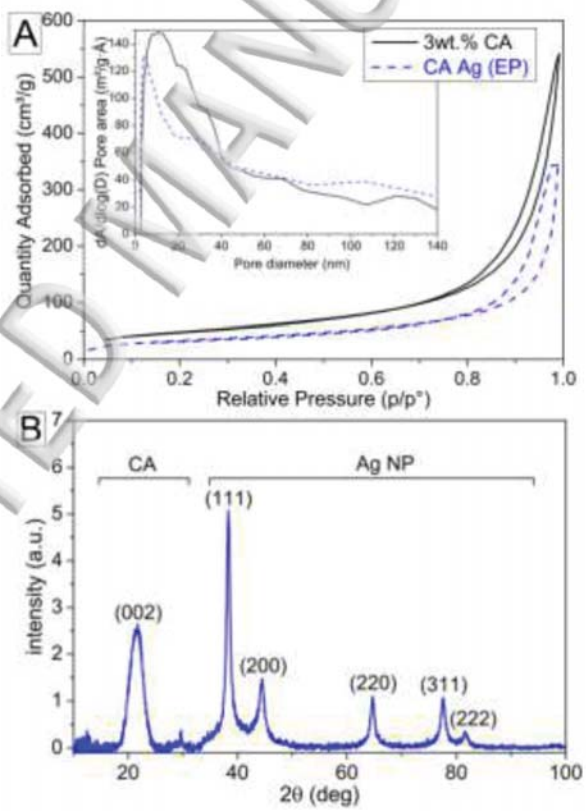

FIG. 2. A) Specific surface area from BET results including BJH inset for the pore size distribution and B) XRD pattern of the CA-Ag composite showing characteristics of both components.

Figure 2A shows physisorption isotherms of the CA and the CA-Ag composite confirming no change in type of physisorption (IUPAC, type IV)[32] and clearly supports the shift to smaller pore sizes from Fig 1. The specific surface area of 170 $m^2\ g^{-1}$ (CA) and 166 $m^2\ g^{-1}$ (CA-Ag) indicate marginal effects on the pore volume. XRD measurements (Fig. 2B) confirm the material composition, showing reflexes of the CA ($2\theta < 35°$) and Ag peaks ($2\theta > 35°$).

To demonstrate the introduced metal functionality, the CA-Ag composite was employed as catalyst in the reduction of 4-nitrophenol by $NaBH_4$.[33] 4-nitrophenolate strongly absorbs light at 400 nm, while the product 4-aminophenolate does not interfere in this spectral region. Accordingly, the reaction progress can be conveniently monitored by UV-Vis absorption spectroscopy (Fig. 3A).

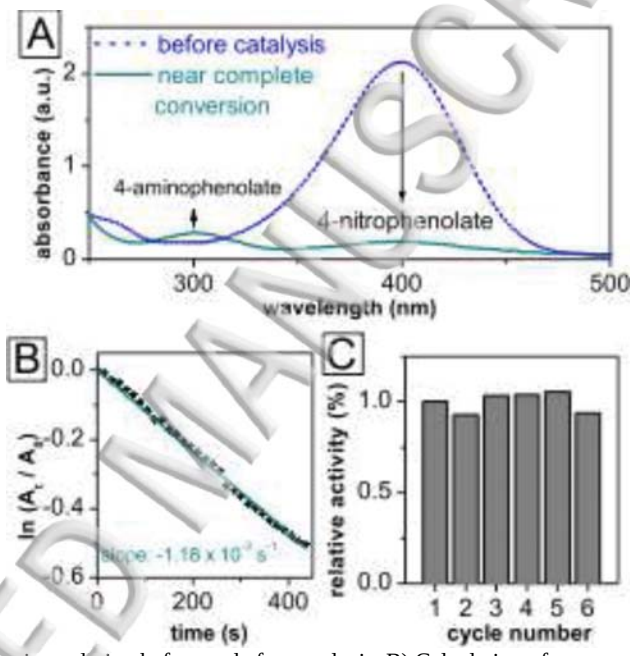

FIG. 3. A) UV-Vis spectra of the reaction solution before and after catalysis. B) Calculation of apparent rate constant, which corresponds to the negative slope of the fit.[33] C) Catalyst activity over several reaction cycles (in % of the initial rate constant).

For the rate constant calculation, the absorbance at 400 nm was determined in intervals of 15 s. 3.36 mg of CA-Ag catalyst was soaked with pure ethanol, which was continuously replaced with reaction solution (60 mM $NaBH_4$ and 0.12 mM 4-nitrophenol in water). The catalytic experiments were performed by transferring the soaked CA-Ag to a quartz cuvette containing 3 mL of fresh reaction solution (no stirring). Given a large excess of $NaBH_4$, the reaction follows a pseudo-first order rate law.[33] This allows us to determine the catalysts' apparent rate constant k_{app} by linearly fitting the natural logarithm of the relative absorbance at 400 nm over time (Fig. 3B). With a k_{app} value of $\approx 1.2 \cdot 10^{-3}\ s^{-1}$, the catalytic activity can compete with colloidal systems such as Ag NP doped carbon spheres ($k_{app} = 1.69 \cdot 10^{-3}\ s^{-1}$),[34] while providing the additional advantage of simple catalyst recovery. As a result of the large surface area of the CA support, the nitrophenol conversion rate markedly exceeds that of Ag NPs on macro-sized cellulose fibers (90 % conversion in approx. 30 min versus only slight conversion

after 1 day).[17] In contrast to other monolith-supported NP systems,[10] the CA-Ag catalyst also exhibits a good aging stability. During 6 reaction cycles, the activity does not decline noticeably (Fig. 3C). The catalyst stability is likely related to the dependable adhesion of the Ag NPs to the cellulose fibrils, which already endured the flow of various solutions in the course of the metallization reaction.

In conclusion, we introduced a modified EP procedure as a facile and sustainable route to functionalize open-porous fibrillar aerogel structures with a homogeneous layer of Ag NPs. The combination of CA supports and EP is strikingly fitting: The polar surface chemistry of the cellulose promotes a dense nucleation and an efficient metal particle attachment, while the conformal deposition is able to utilize the complex aerogel structure. As we have shown in a catalytic model reaction, the hybrid biopolymer-metal material combines the functionality of the metal NPs with the benefits of the CA support. This approach will be extended to other metals (Au, Pt) and other substrate aerogels to realize aerogel-metal composites of varying morphology to be employed in plasmonic, sensing and catalytic applications.

ACKNOWLEDGMENTS

Thanks are due to Dr. René Tannert for fruitful discussion, Dr. Klemens Kelm and Philipp Watermeyer for TEM analysis, Alexander Francke for XRD analysis, Dr. Umme Habiba Hossain for support with the Ag deposition, and Eva-Maria Felix for help with the UV-Vis measurements.

REFERENCES

[1]C. Zhu, D. Du, A. Eychmüller, and Y. Lin, Chem. Rev., **115**, 8896 (2015).

[2]F. Muench, D. M. De Carolis, E.-M. Felix, J. Brötz, U. Kunz H.-J. Kleebe, S. Ayata, C. Trautmann, and W. Ensinger, Chem. Plus Chem., **80**, 1448 (2015).

[3]B. C. Tappan, S. A. Steiner III, and E. P. Luther, Angew. Chem. Int. Ed., **49**, 4544 (2010).

[4]Z. Qi, and J. Weissmüller, ACS Nano, **7**, 5948 (2013).

[5]A. Mikhalchan, Z. Fan, T. Q. Tran, P. Liu, V. B. C. Tan, T.-E. Tay, H. M. Duong, Carbon, **102**, 409 (2016).

[6]G. Nyström, M. P. Fernández-Ronco, S. Bolisetty, M. Mazzotti, and R. Mezzenga, Adv. Mater., **28**, 472 (2016).

[7]P. Trogadas, V. Ramani, P. Strasser, T. F. Fuller, and M.-O. Coppens, Angew. Chem. Int. Ed., **55**, 122 (2016).

[8]Z. Shi, G. O. Phillips, and G. Yang, Nanoscale, **5**, 3194 (2013).

[9]J. W. Long, B. Dunn, D. R. Rolison, and H. S. White, Chem. Rev., **104**, 4463 (2004).

[10]N. Moitra, K. Kanamori, Y. H. Ikuhara, X. Gao, Y. Zhu, G. Hasegawa, K. Takeda, T. Shimada, and K. Nakanishi, J. Mater. Chem. A, **2**, 12535 (2014).

[11]J. Tang, Z. Shi, R. M. Berry, and K. C. Tam, Ind. Eng. Chem. Res., **54**, 3299 (2015).

[12]B. J. Murray, E. C. Walter, and R. M. Penner, Nano Lett., **4**, 665 (2004).

[13]E. Kim, N.S. Arul, L. Yang, and J. I. Han, RSC Adv., **5**, 76729 (2015).

[14]B. Kim, S.C. Hong, S. Jung, J. Nam, J. Bang, and S. Kim, Chem. Phys. Chem., **14**, 2663 (2013).

[15]V. Garcia-Gradilla, S. Sattayasamitsathit, F. Soto, F. Kuralay, C. Yardimci, D. Wiitala, M. Galarnyk, and J. Wang, Small, **10**, 4154 2014.

[16]N. D. Luong, Y. Lee, and J.-D. Nam, Eur. Polym. J., **44**, 3116 (2008).

[17]S. Ashraf, S. Rehman, F. Sher, Z. M. Khalid, M. Mehmood, and I. Hussain, Cellulose, **21**, 395 (2014).

[18]S. Vivekanandhan, L. Christensen, M. Misra, and A. K. Mohanty, J. Biomater. Nanobiotechnol., 3, 371 (2012).

[19]J. T. Korhonen, P. Hiekkataipale, J. Malm, M. Karppinen, O. Ikkala, and R. H. A. Ras, ACS Nano, **5**, 1967 (2011).

[20]J. W. Elam, J. A. Libera, M. J. Pellin, A. V. Zinovev, J. P. Greene, and J. A. Nolen, Appl. Phys. Lett. **89**, 053124 (2006).

[21]K. Liu, Y.-M. Chen, G. M. Policastro, M. L. Becker, and Y. Zhu, ACS Nano, **9**, 6041 (2015).

[22]E.-M. Felix, F. Muench, and W. Ensinger, RSC Adv., **4**, 24504 (2014).

[23]Q. Zhou, K. Zhong, W. Fu, Q. Huang, Z. Wang, and B. Nie, Chem. Eng. J., **270**, 320 (2015).

[24]F. Muench, E. Eils, M. E. Toimil-Molares, U. H. Hossain, A. Radetinac, C. Stegmann, U. Kunz, S. Lauterbach, H.-J. Kleebe, and W. Ensinger, Surf. Coat. Technol., **242**, 100 (2014).

[25]X. Wu, C. Lu, W. Zhang, G. Yuan, R. Xiong, and X. Zhang, J. Mater. Chem. A, **1**, 8645 (2013).

[26]H. Qi, J. Liu, J. Pionteck, P. Pötschke, and E. Mäder, Sens. Act. B: Chem., **213**, 20 (2015).

[27]S. Wang, A. Lu, and L. Zhang, Prog. Polym. Sci., **53**, 169 (2016).

[28]H. Jin, Y. Nishiyama, M. Wada, and S. Kuga, Colloids Surf. A: Physicochem. Eng. Asp., **240**, 63 (2004).

[29]I. Karadagli, B. Schulz, M. Schestakow, B. Milow, T. Gries, and L. Ratke, J. Supercrit. Fluid, **106**, 105 (2015).

[30]S. Hoepfner, L. Ratke, and B. Milow, Cellulose, **15**, 121 (2008).

[31]M. Schestakow, I. Karadagli, and L. Ratke, Carbohyd. Polym., **137**, 642 (2016).

[32]K. Sing, D. Everett, R. Haul, L. Moscou, R. Pierotti, J. Rouquerol, and T. Siemieniewska, Pure & Appl. Chem., **57**, 603 (1985).

[33]P. Hervés, M. Pérez-Lorenzo, L. M. Liz-Marzán, J. Dzubiella, Y. Lu, and M. Ballauff, Chem. Soc. Rev., **41**, 5577 (2012).

[34]S. Tang, S. Vongehr, and X. Meng, J. Phys. Chem. C, **114**, 977 (2010).